The Journal of Immunology



# The Encephalitogenic, Human Myelin Oligodendrocyte Glycoprotein–Induced Antibody Repertoire Is Directed toward Multiple Epitopes in C57BL/6-Immunized Mice

Pankaj Bansal, Tarique Khan, Uta Bussmeyer, Dilip K. Challa, Rafal Swiercz, Ramraj Velmurugan, Raimund J. Ober and E. Sally Ward

*J Immunol* 2013; 191:1091-1101; Prepublished online 1 July 2013;
doi: 10.4049/jimmunol.1300019
http://www.jimmunol.org/content/191/3/1091



*The Journal of Immunology* is published twice each month by
The American Association of Immunologists, Inc.,
9650 Rockville Pike, Bethesda, MD 20814-3994.

Print ISSN: 0022-1767 Online ISSN: 1550-6606.

# The Encephalitogenic, Human Myelin Oligodendrocyte Glycoprotein–Induced Antibody Repertoire Is Directed toward Multiple Epitopes in C57BL/6-Immunized Mice

**Pankaj Bansal,* Tarique Khan,* Uta Bussmeyer,* Dilip K. Challa,* Rafal Swiercz,* Ramraj Velmurugan,* Raimund J. Ober,*,† and E. Sally Ward***

**Although Abs specific for myelin oligodendrocyte glycoprotein (MOG) have been detected in patients with multiple sclerosis (MS), their contribution to pathogenesis remains poorly understood. Immunization of C57BL/6 mice with recombinant human MOG (hMOG) results in experimental autoimmune encephalomyelitis involving MOG-specific, demyelinating Abs. This model is therefore informative for understanding anti-MOG humoral responses in MS. In the current study, we have characterized the hMOG-specific Ab repertoire in immunized C57BL/6 mice using both in vitro and in vivo approaches. We demonstrate that hMOG-specific mAbs are not focused on one specific region of MOG, but instead target multiple epitopes. Encephalitogenicity of the mAbs, assessed by the ability of the mAbs to exacerbate experimental autoimmune encephalomyelitis in mice, correlates with the activity of the mAbs in binding to CNS tissue sections, but not with other in vitro assays. The targeting of different MOG epitopes by encephalitogenic Abs has implications for disease pathogenesis, because it could result in MOG cross linking on oligodendrocytes and/or immune complex formation. These studies reveal several novel features concerning pathogenic, humoral responses that may have relevance to human MS.** ***The Journal of Immunology*****, 2013, 191: 1091–1101.**

Multiple sclerosis (MS) is a demyelinating, inflammatory disease of the CNS that is characterized by infiltrates of macrophages, T, and B cells (1, 2). Although much evidence supports the contribution of autoreactive Abs to pathogenesis in a significant subset of MS patients, the nature of these Abs and how they participate in the disease process remains poorly understood (3, 4). Abs recognizing myelin oligodendrocyte glycoprotein (MOG) are of particular relevance because the extracellular Ig V-like domain of MOG is exposed on the outer lamellae of the myelin sheath (5, 6), providing an appropriate target for Ab-mediated attack. Anti-MOG humoral responses in MS patients, nonhuman primates (marmosets), and rodent models of MS have therefore been extensively studied (3, 4, 7–14). However, the analysis of anti-MOG responses in humans has led to inconsistent results (3, 4, 8–16). This is further confounded by the presence of anti-MOG Abs in normal human controls combined with the use of MOG of different derivations in binding assays and variations in the tissues or body fluids analyzed (3, 4, 8–13, 15, 16). Consequently, in addition to limited knowledge concerning the demyelinating, anti-MOG repertoire, it remains a challenge to distinguish pathogenic from nonpathogenic, MOG-specific Abs.

MOG-specific Abs that are elicited following immunization of BALB/c or SJL/J mice with rodent (mouse/rat) MOG or brain extract can have demyelinating activity (7, 17–19). For example, Abs such as the extensively characterized mouse monoclonal, 8-18C5, exacerbate experimental autoimmune encephalomyelitis (EAE) when transferred into autoantigen-immunized rats or mice (20, 21). A feature of pathogenic, demyelinating Abs in both rodents and nonhuman primates (marmosets) is that they recognize native, but not denatured, MOG (7, 11, 18, 22, 23). Significantly, MOG recognition by demyelinating Abs induced by immunization of mice with MOG (rat, mouse, or bovine) has been reported to be critically dependent on residues in an exposed loop (the FG loop in the Ig V-like domain) of this autoantigen, leading to the conclusion that in rodents the pathogenic humoral response to MOG is centered on one immunodominant region (7).

By contrast with BALB/c or SJL/J mice (7, 17–19), immunization of C57BL/6 mice with rat MOG (rMOG), which shares 95% homology with mouse MOG (mMOG), induces EAE that is B cell independent and does not involve a demyelinating Ab response (24–26). Interestingly, in human MOG (hMOG)-immunized C57BL/6 mice, EAE is dependent on B cells (24, 27, 28). Significantly, this B cell dependence is due to the induction of demyelinating anti-MOG Abs that recognize native MOG (22), rather than a contribution of B cells to Ag presentation (24, 27). These observations have motivated studies directed toward understanding how the immune response to human versus rodent MOG differs in C57BL/6 mice. For both hMOG and mMOG/rMOG, the immunodominant T cell epitope is contained within residues 35–55 (27). Rodent MOG differs from hMOG by a proline to serine replacement at residue 42 within this epitope. Studies in C57BL/6 mice have demonstrated that hMOG35–55 is less effective in inducing encephalitogenic T cells relative to the corresponding rat epitope (27). For the humoral response, although Ab titers against recombinant mMOG have been shown to

*Department of Immunology, University of Texas Southwestern Medical Center, Dallas, TX 75390; and †Department of Electrical Engineering, University of Texas at Dallas, Richardson, TX 75080

Received for publication January 4, 2013. Accepted for publication June 3, 2013.

This work was supported in part by a grant from the National Multiple Sclerosis Society (RG 4308).

Address correspondence and reprint requests to Dr. E. Sally Ward, Department of Immunology, University of Texas Southwestern Medical Center, 6000 Harry Hines Boulevard, Dallas, TX 75390. E-mail address: sally.ward@utsouthwestern.edu

The online version of this article contains supplemental material.

Abbreviations used in this article: DPBS, Dulbecco's PBS; EAE, experimental autoimmune encephalomyelitis; hMOG, human myelin oligodendrocyte glycoprotein; mMOG, mouse myelin oligodendrocyte glycoprotein; MOG, myelin oligodendrocyte glycoprotein; MS, multiple sclerosis; OL, oligodendrocyte; rMOG, rat myelin oligodendrocyte glycoprotein; RT, room temperature; RU, resonance unit; SPR, surface plasmon resonance.



www.jimmunol.org/cgi/doi/10.4049/jimmunol.1300019

be similar in mice immunized with recombinant hMOG or rMOG (27), demyelinating activity and recognition of native, glycosylated MOG on oligodendrocytes (OLs) is only observed following hMOG, but not rMOG, delivery (22, 26, 27). Mutation of residue 42 (proline) in recombinant hMOG to serine recapitulates the activity of rMOG/mMOG, including B cell–independent disease (22, 27). This single amino acid change therefore results in a fundamental difference in both the T and B cell components of the MOG-specific immune response following immunization of C57BL/6 mice with rodent or hMOG, although the mechanism for this remains incompletely understood. Nevertheless, hMOG-induced EAE in C57BL/6 mice represents an instructive model for the significant proportion of MS patients in whom Abs are believed to play a role in pathogenesis (29–31).

To date, the properties of the MOG-specific Ab repertoire following immunization of mice with hMOG are poorly characterized. With the concept that hMOG-induced EAE is informative for better understanding pathogenic, humoral responses in MS, the current study is directed toward addressing this issue. A panel of mAbs has been generated from hMOG-immunized C57BL/6 mice. The binding properties of these mAbs for both hMOG and mMOG have been analyzed. By contrast with earlier studies of demyelinating, MOG-specific Abs in BALB/c or SJL/J mice (7), these mAbs are not dependent on residues 103 and 104 in the exposed FG loop of MOG for recognition. The analysis of the ability of the mAbs to exacerbate EAE in a transfer model has allowed correlates between encephalitogenicity and in vitro binding activities to be made. The disease-exacerbating mAbs can be consistently identified by their ability to recognize native MOG in CNS tissue sections, but not by other in vitro assays. Significantly, these mAbs recognize at least four distinct epitopes of MOG, indicating a diverse repertoire. This diversity has implications for disease mechanism, because it would enable MOG cross linking and consequent signaling effects that have been suggested to play a role in demyelination (32, 33). Collectively, these studies therefore define novel properties for pathogenic, MOG-specific mAbs that could have relevance to human disease.

## Materials and Methods

### *Mice*

Female C57BL/6 mice were purchased from The Jackson Laboratory (Bar Harbor, ME) and used at 9 to 10 wk of age. Mice were housed in the animal facility at University of Texas Southwestern Medical Center and handled according to protocols approved by the Institutional Animal Care and Use Committee.

### *Generation of transfectants expressing 8-18C5*

The $V_H$ and $V_L$ domain genes of the 8-18C5 Ab (Protein Data Bank code 1PKQ) (34) were synthesized (Genscript USA, Piscataway, NJ). The leader peptide of the Ig H (MAVLVLFLCLVAFPSCVLS) and L chain (MKLPVRLLVLMFWIPASSS) genes corresponding to the leader peptide sequences for the D1.3 hybridoma (35) were appended to the 5′ ends of the $V_H$ and $V_L$ genes, respectively, using two rounds of PCR with overlapping oligonucleotides. The genes encoding the C region genes [mouse IgG1, κ; derived from anti-lysozyme D1.3 hybridoma cells (35)] were appended to the 3′ ends of the $V_H$ and $V_L$ domain genes, respectively, using designed oligonucleotides and splicing by overlap extension (36). The PCR products encoding the complete 8-18C5 H and L chain genes were cloned into pOptiVEC-TOPO and pcDNA 3.3-TOPO (OptiCHO Ab express kit; Life Technologies, Grand Island, NY), respectively.

The 8-18C5 L chain expression construct was transfected into CHO/DG44 cells by electroporation. Following selection of stably transfected clones in CD/DG44 CHO medium containing 500 μg/ml geneticin (without HT supplement), CHO/DG44 clones expressing the highest levels of 8-18C5 L chain were identified by ELISA using a goat anti-mouse Cκ–HRP conjugate (Jackson ImmunoResearch Laboratories, West Grove, PA) for detection. The highest expressing cells were cloned by limiting dilution and transfected with the 8-18C5 H chain expression plasmid. Stably transfected clones were selected in Opti-CHO medium (Life Technologies) containing 500 μg/ml geneticin and screened for expression of 8-18C5 Ab using ELISA and mMOG-coated 96-well plates (see below for ELISA protocol). The CHO/DG44 clones that expressed the highest levels of Ab were subsequently cultured in increasing concentrations of methotrexate (50 nM–4 μM) to induce methotrexate-induced gene amplification. For large-scale expression of the 8-18C5 Ab, cells were grown in shake flasks (75 rpm) in a 5% $CO_2$ incubator in Opti-CHO medium. 8-18C5 mAb was purified from culture medium using protein G-Sepharose (GE Healthcare Biosciences, Piscataway, NJ) and purity analyzed by SDS-PAGE. For use in mice, CHO/DG44 transfectants expressing the 8-18C5 mAb were expanded and Ab purified using protein G-Sepharose by BioXCell (West Lebanon, NH).

### *Expression of recombinant MOG*

An analogous construct design to that described previously for the production of the extracellular domain of hMOG1–121 (37) was used to generate an expression plasmid for recombinant mMOG. A synthetic gene encoding the N-terminal 121 residues of the extracellular domain of mMOG with codons encoding a hexahistidine tag at the C terminus and honey bee mellitin signal peptide (38) at the N terminus was synthesized (Genscript USA) with EcoRI and NotI sites appended and cloned into EcoRI-NotI–digested pVL1393 (BD Biosciences, San Diego, CA). To generate a construct to express the mMOG mutant (mMOG-DM, containing H103A, S104E), designed oligonucleotides combined with splicing by overlap extension (36) were used, and the resulting PCR product was cloned into pVL1393 as an EcoRI-NotI fragment. Expression constructs were cotransfected into *Sf9* cells together with Baculogold linearized baculovirus DNA (BD Biosciences, San Diego, CA), and high-titer virus stocks were generated. High Five (Life Technologies) insect cells were infected with mMOG and mMOG-DM baculoviral stocks and respective recombinant proteins purified from the supernatant using $Ni^{2+}$-NTA agarose (Qiagen, Valencia, CA) and standard methods. Purified proteins were dialyzed into 20 mM ammonium bicarbonate (pH 8) and lyophilized for storage at −20°C.

Baculoviral stock for the expression of the extracellular domain (residues 1–121) of hMOG (24, 37) was generously provided by Drs. Anne Cross and Jeri-Anne Lyons (Washington University School of Medicine). hMOG protein was isolated using the same methods as for mMOG.

### *Immunization of mice with MOG and hybridoma generation*

Female C57BL/6 mice were immunized s.c. with the extracellular domain of hMOG (200 μg/mouse) emulsified in CFA (Sigma-Aldrich, St. Louis, MO). Animals were divided into two groups of four mice each. One group was boosted s.c. once after 2 wk of primary immunization with recombinant hMOG (200 μg/mouse) emulsified in IFA (Sigma-Aldrich). Seven days postimmunization, mice with the highest Ab titers specific for hMOG (determined by ELISA) were selected. The following day, spleens, lymph nodes, and bone marrow were removed aseptically from euthanized mice. The separated organs were teased apart in DMEM medium (Lonza, Walkersville, MD) and passed through cell strainers (70 μm; BD Biosciences) to obtain single-cell suspensions. Sp2/0-Ag14 cells (maintained at the logarithmic phase of growth) were fused with single-cell suspensions following standard protocols (39) or using ClonaCell-HY Kit (StemCell Technologies, Vancouver, Canada). Twelve days postfusion, supernatants from culture wells were analyzed for the production of Abs against hMOG by ELISA. Hybridomas from positive wells were cloned by limiting dilution to obtain stable hybrid single-cell clones secreting anti-hMOG mAbs.

To analyze serum anti-MOG responses, C57BL/6 mice (four mice per group) were immunized s.c. with recombinant hMOG or mMOG (200 μg/mouse) as above. Serum samples were collected at days 8, 11, 13, and 22 postimmunization.

### *Purification of mAbs*

Hybridomas were cultured in either cDMEM containing 10% IgG-depleted FCS (by passage over protein G-Sepharose) or Hybridoma SFM (serum-free medium; Life Technologies). All mAbs were purified from culture supernatants of hybridomas using protein G-Sepharose (GE Healthcare Life Sciences) and standard methods. The anti-lysozyme mAb D1.3 (35) was purified using lysozyme-Sepharose (40). Eluted mAbs were dialyzed against Dulbecco's PBS (pH 7.4; Lonza), harvested, and concentrated. Protein concentrations were determined by BCA (ThermoFisher Scientific, Rockford, IL). The purity of each mAb was assayed by SDS-PAGE. Several mAbs (1002, 1003, and 1023) were also cultured and purified using protein G-Sepharose by BioXCell.

### *ELISA*

Hybridoma supernatants, purified mAbs (1 μg/ml), or serum dilutions were analyzed for binding to hMOG, mMOG, and mMOG-DM using ELISA and standard protocols. The 96-well plates were coated with recombinant proteins at a concentration of 10 μg/ml. Bound mAbs were detected using rabbit anti-mouse Ig conjugated to HRPO (Life Technologies).

The isotypes of the mAbs were determined using a mouse mAb isotyping kit (Sigma-Aldrich) following a standard protocol with recombinant hMOG-coated 96-well plates. Incubation with mAb was followed by the addition of goat anti-mouse isotype-specific Abs at 1:1000 dilutions. Bound isotype-specific Abs were detected using rabbit anti-goat IgG-HRPO conjugates (Sigma-Aldrich).

### *Isolation of Ig variable domain genes from hybridomas*

RNA was isolated and used in cDNA syntheses with oligo(dT) or the following forward oligonucleotide primers (mCH1for: 5′-CTT GAC CAG GCA TCC CAG GGT CAC-3′; mCκfor: 5′-GAA GTT GTT CAA GAA GCA CAC GAC-3′) that anneal ~70–90 bp from the 5′ end of CH1 and Cκ genes, respectively (41). mCH1for anneals to both IgG1 and IgG2b CH1 regions, although there is a one codon mismatch for IgG2b (41). cDNA was used in PCRs with previously described oligonucleotides specific for mouse $V_H$ and $V_L$ domain genes (42–44) or a primer mix (45) for amplification of $V_H$ and $V_L$ domain genes (generously provided by Dr. G. Georgiou, University of Texas Austin, Austin, TX) using standard methods of molecular biology. PCR products were gel-purified and either sequenced directly or ligated into pGEM-T (Promega, Madison, WI) to generate clones from which plasmid DNA was extracted for sequencing.

### *Affinity measurements and competition binding assays*

The dissociation constants ($K_d$s) for the interactions of the mAbs with mMOG, hMOG, and mMOG-DM were determined using a BIAcore 2000 (GE Healthcare Bioscience, Uppsala, Sweden). Recombinant mMOG, hMOG, and mMOG-DM were covalently immobilized on CM5 sensor chips in 10 mM sodium acetate buffer (pH 4.8) using amine-coupling kit reagents supplied by the manufacturer. The immobilization densities for mMOG, hMOG, and mMOG-DM were in the range of 300–700 resonance units (RU). Binding studies were conducted at 25°C using PBS (pH 7.4) containing 0.01% Tween and 0.05% sodium azide as running buffer. All mAbs were injected as analyte using a range of concentrations at flow rates of 10 μl/min. Regeneration of the sensor surface between analyte injections was achieved by injection of 0.15 M NaCl/0.1 M glycine-HCl (pH 2.8). Experiments were carried out using programmed methods and randomized repeat injections to ensure that there was no significant loss of ligand-binding activity during the course of the experiment (46). Data were fitted using custom written software to determine $K_d$ values (46, 47). All $K_d$ values are apparent, rather than absolute, due to bivalent binding of Ab to immobilized MOG.

For competition binding assays, mAbs 1002, 1003, 1005, 1011, 1012, or 8-18C5 and recombinant mMOG were immobilized on flow cells of CM5 chips to densities ranging from 940–3038 RU (mAbs) and 537–946 RU (mMOG), respectively. Recombinant mMOG (200 nM) was injected at a flow rate of 10 μl/min. This injection was followed by injection of each mAb at a concentration of ~5 times its $K_d$ value at a flow rate of 10 μl/min. The anti-lysozyme Ab D1.3 [mouse IgG1 (35)] was used as a negative control in these assays. The sensor surface was regenerated as described above.

### *Flow cytometry*

The binding of anti-hMOG Abs (mAbs or serum samples) to surface-expressed mouse MOG on transfected EL4 cells (EL4-MOG) (23) was assayed using flow cytometry and a FACSCalibur (BD Biosciences). EL4-MOG and untransfected EL4 cells were generously provided by Dr. Gurumoorthy Krishnamoorthy (Max Planck Institute of Neurobiology, Martinsreid, Germany). Cells ($3 \times 10^6$) were incubated with either sera (1:100 dilution) from hMOG- or mMOG-immunized mice (harvested at day 22 post-immunization) or 50 μg/ml mAb. Bound Ab was detected using goat anti-mouse IgG (H+L)-Alexa Fluor 647 (Life Technologies). As controls, untransfected EL4 cells and the anti-lysozyme Ab D1.3 (35) were used.

### *Exacerbation of EAE*

C57BL/6 mice were immunized s.c. at four sites in the flanks with 100 μg hMOG35–55 peptide emulsified with CFA (Sigma-Aldrich) supplemented with an additional 4 mg/ml heat-inactivated *Mycobacterium tuberculosis* (strain H37RA; Difco). A total of 200 ng pertussis toxin (List Biological Laboratories, Campbell, CA) was injected i.p. on days 0 and 2. The mice were monitored daily for clinical signs of EAE. On day 15, the mice that had EAE scores of 0–3.5 were sorted into groups of eight mice per treatment. The sorting of mice into groups was carried out using a cost function (implemented in MATLAB) based on EAE scores on each day prior to and including day 15, resulting in equal numbers of mice with similar disease course in each group. This cost function takes into account the similarity (in average scores and covariance) and the SD of the disease scores up to and including day 15. A low proportion of mice developed EAE with scores >3.5 (at day 15) and were excluded from the experiments. Mice were injected i.v. with 200 μg of each mAb, isotype control D1.3 [mouse IgG1, anti-lysozyme (35)], or DPBS (control) and monitored daily for clinical signs of EAE for 35 d postimmunization as described previously (48). Data are presented as mean clinical scores for each group, and dead animals were given a score of 6 from the day of death onwards. The activity of each MOG-specific mAb was analyzed in at least two independent experiments.

### *Immunofluorescence staining of the spinal cord and data analysis*

For use in immunohistochemistry, anti-MOG mAbs were directly labeled with Alexa 555 or Alexa 647 carboxylic acid, succinimidyl ester (Invitrogen) using previously described methods (49). The degrees of labeling (molar ratio of dye molecules per Ab molecule) for each mAb were determined using standard methods.

C57BL/6 mice or hMOG35–55 peptide-immunized C57BL/6 mice (as above) with EAE scores of 3 to 4 at day 15 postimmunization were perfused with 10 U/ml heparinized DPBS, followed by surgical removal of spinal cords or, for normal mice only, livers. Tissues were immediately snap-frozen in liquid nitrogen and stored at −80°C. Tissues were embedded in Tissue-Tek OCT compound (Sakura Finetek USA, Torrance, CA), sectioned (4-μm thick) using a Leica cryotome (Leica Microsystems), and stored at −80°C. Tissue sections were air-dried and fixed in cold (−20°C) acetone. Fixed sections were air-dried at room temperature (RT) and rehydrated in DPBS (Lonza) and blocked with 5% BSA/DPBS for 1 h at RT followed by incubation with Fcγ receptor blocking Ab (2.4G2) at 5 μg/ml in 1% BSA/DPBS for 15 min at RT. Sections were incubated with 50 μg/ml Alexa 555–labeled mAbs in 1% BSA/DPBS at RT for 45 min. Spinal cords were costained with 8 μg/ml Alexa 647–labeled anti-OL O1 Ab (eBioscience, San Diego, CA) that binds to galactocerebroside. Liver sections were stained with either Alexa 555–labeled mAbs or 2.5 μg/ml rat anti-CD31 Ab (clone 390; Abcam, Cambridge, MA) followed by Alexa 555–labeled goat anti-rat IgG. For competition binding assays with 8-18C5 mAb, tissue sections were preincubated for 45 min with 200 μg/ml 8-18C5 prior to addition of 50 μg/ml mAb for an additional 45 min. For colocalization analyses, sections were incubated with 5 μg/ml 8-18C5 and 50 μg/ml mAb 1005 for 60 min. Sections were washed with DPBS and mounted in Vectashield hard-set mounting medium with DAPI (Vector Laboratories, Burlingame, CA). As negative controls, Alexa 555–labeled isotype matched Abs were used.

Tissue sections were imaged using a Zeiss Axiovert 200M inverted microscope that was equipped with a Zeiss 63×, 1.4 NA Plan-Apochromat objective lens (Carl Zeiss) and an ORCA CCD camera (Hamamatsu, Bridgewater, NJ). Images were acquired with filtersets specific for Alexa Fluor 555 (TRITC-B-000-ZERO; Semrock, Rochester, NY), Alexa 647 Fluor (Cy5-4040C-ZERO; Semrock, Rochester, NY), and DAPI (part number 31013v2; Chroma Technologies, Bellows Falls, VT). The data were processed and displayed using the microscopy image analysis tool (MIATool) software package (www4.utsouthwestern.edu/wardlab/miatool.asp) in MATLAB (Mathworks). The acquired images were embedded in 16-bit grayscale format and overlaid for presentation. For comparative purposes, in Figs. 6A, 6B, and 7B, the intensities of the individual channels were adjusted in an analogous manner within each of the datasets. For Fig. 7C and Supplemental Fig. 2, intensities were adjusted individually for each image to optimize visualization of the staining patterns of the mAbs. Images were exported into Adobe Photoshop CS6 (Adobe Systems) for final composition of the figures.

### *Statistical analyses*

Statistical analyses of differences in mean clinical score between groups of mAb-treated mice and control mice were carried out using Student *t* test in the statistics toolbox of MATLAB (Mathworks). The $p$ values $<0.05$ were taken to be significant.

## Results

### *Isolation of MOG-specific hybridomas from C57BL/6 mice*

Immunization of C57BL/6 mice with recombinant hMOG is known to result in EAE, in which demyelinating Abs play a role in

pathogenesis (22, 28). Toward characterizing the MOG-specific Ab repertoire in hMOG-immunized mice, 15 hybridomas that secreted mAbs with binding specificity for recombinant hMOG were generated (Fig. 1A). None of the mAbs share both $V_H$ and $V_L$ domain sequences, although several have the same $V_H$ domain sequence with different $V_L$ (mAb 1012 or 1021) or the same $V_L$ domain sequence with different $V_H$ (1003, 1012; 1002, 1013) (Supplemental Fig. 1). Comparison of the Ab V region sequences with those of the MOG-specific 8-18C5 mAb [isolated from BALB/c mice (17)] demonstrates that none of the mAbs share the same $V_H$ or $V_L$ sequence with this demyelinating Ab (Supplemental Fig. 1). All mAb L chains are κ. In addition, both sequencing and ELISA analyses indicated that four of the mAbs (1004, 1005, 1009, and 1014) are of the IgG2b isotype, with the remainder of the IgG1 subclass (data not shown).

We further investigated whether the mAbs cross-reacted with mMOG, the relevant autoantigen for EAE in mice. Using ELISAs, the majority of the mAbs (9 out of 15) showed strong reactivities toward mMOG (Fig. 1B), although four (mAbs 1003, 1013, 1014, and 1019) bound weakly. Two of the mAbs (1001 and 1021) gave background levels of signal. Earlier studies in BALB/c and SJL/J mice have demonstrated that immunization with rodent or bovine MOG generates Abs, including the well-characterized mAb 8-18C5, that are dependent on residues 103 and 104 in an exposed loop linking the F and G Ig-like domain strands (the FG loop) of MOG for recognition (7). This prompted us to analyze the ability of the MOG-specific mAbs to interact with a mutated mMOG variant (mMOG-DM) in which residues 103 (His) and 104 (Ser) were changed to alanine and glutamic acid, respectively. Unexpectedly, all mAbs showed similar levels of binding to both wild-type mMOG and mMOG-DM (Fig. 1B). Consistent with earlier studies (7), the previously characterized mAb, 8-18C5, is highly dependent on residues 103 and 104 for recognition (Fig. 1B).

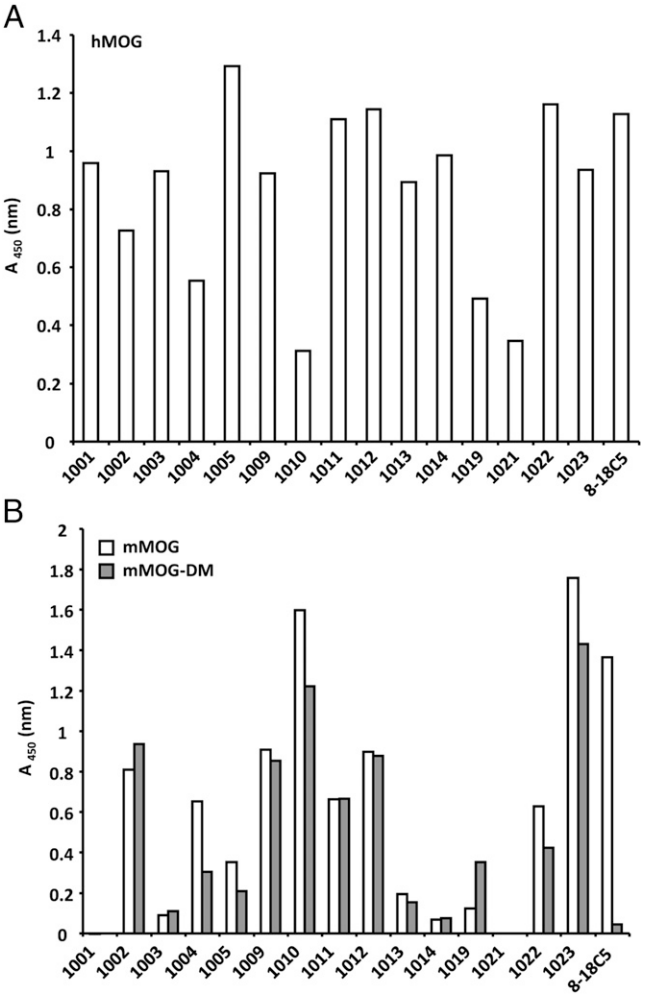


**FIGURE 1.** Binding of mAbs to recombinant hMOG (**A**), mMOG (**B**), or mMOG-DM (B) using ELISAs with Ag-coated plates. mAbs were used at a concentration of 1 μg/ml, and bound mAbs were detected with anti-mouse HRPO conjugate. Background OD values (signal using BSA-coated plates) were subtracted from all OD (450 nm) values obtained with Ag-coated plates. Means of duplicate values are shown, and data are representative of at least three independent experiments. As a control, binding by the anti-MOG mAb 8-18C5 is also shown.

### *Surface plasmon resonance analyses of the Ab–MOG interactions*

The observation that mutation of residues 103 and 104 of MOG did not ablate recognition by the mAbs prompted us to determine their binding affinities for mMOG, hMOG, and mMOG-DM using surface plasmon resonance (SPR). To mimic the multivalent exposure of MOG on OLs, these studies were carried out with immobilized MOG (human or mouse) on the sensor chip and mAbs in solution, resulting in the determination of apparent equilibrium dissociation constants.

Consistent with the ELISA data, the binding of mAbs 1001 and 1021 to mMOG was undetectable, and these were not analyzed further (data not shown). All other mAbs bound with measurable affinities to both hMOG and mMOG (Table I), with the exception of mAbs 1013, 1014, and 1019, for which the low affinities (>0.5 μM) for either all MOG species (mAbs 1014 and 1019) or for mMOG/mMOG-DM (mAb 1013) precluded accurate determination under the conditions of the SPR experiments. For the majority of the higher affinity mAbs, the dissociation constants were congruent with the ELISA data for mMOG and mMOG-DM (Fig. 1B), although the affinities of 17 and 21 nM for mAb 1003 for these two proteins, respectively, did not correlate well with the low ELISA signal. Conversely, binding of mAb 1005 to hMOG in ELISAs is relatively strong (Fig. 1A) despite its comparatively low affinity for hMOG in SPR (38 nM). Importantly, six mAbs (1002, 1004, 1009, 1010, 1012, and 1023) had similar affinities for mMOG, hMOG, and mMOG-DM, demonstrating that they recognized a common epitope across species and were unaffected by mutation of residues 103 and 104. Although mAbs 1003, 1005, 1011, and 1022 had higher affinity for hMOG relative to mMOG, their affinities for mMOG and

Table I. Apparent $K_d$s for MOG-specific mAbs

| mAb | Isotype | hMOG $K_d$ (nM) | mMOG $K_d$ (nM) | mMOG-DM $K_d$ (nM) |
|---|---|---|---|---|
| 1002 | IgG1 | 3.3 | 4.5 | 5.0 |
| 1003 | IgG1 | 2.9 | 17.0 | 21.0 |
| 1004 | IgG2b | 4.8 | 5.4 | 4.2 |
| 1005 | IgG2b | 38.0 | 301.0 | 321.0 |
| 1009 | IgG2b | 1.4 | 1.0 | 1.5 |
| 1010 | IgG1 | 1.0 | 0.9 | 0.5 |
| 1011 | IgG1 | 1.2 | 7.5 | 8.7 |
| 1012 | IgG1 | 5.0 | 3.4 | 3.4 |
| 1013 | IgG1 | 8.7 | ND | ND |
| 1022 | IgG1 | 14.6 | 37.0 | 39.0 |
| 1023 | IgG1 | 0.7 | 1.0 | 1.2 |
| 8-18C5 | IgG1 | 10.6 | 18.6 | ND |

ND, Apparent affinities too low to be determined.

mMOG-DM were indistinguishable. Thus, mutation of residues 103 and 104 does not impact the binding of any of the mMOG-specific mAbs. By contrast, but consistent with both our ELISA results and the observations of others (7), 8-18C5 bound to both hMOG and mMOG but with immeasurably low affinity (under the conditions of assay) to mMOG-DM in SPR experiments.

Although none of the mAbs were dependent on residues 103 and 104 in the FG loop of mMOG for recognition, it remained possible that they could compete with 8-18C5 for binding to MOG. We therefore used SPR to investigate this. 8-18C5 was immobilized on the sensor chip, followed by injections of mMOG (200 nM) and then each anti-MOG mAb (at a concentration of ~5 times the equilibrium dissociation constant). We reasoned that no or limited competition with 8-18C5 would sandwich the MOG between 8-18C5 and injected mAb, whereas competition would result in no interaction of the mAb with the preformed MOG/8-18C5 complex. mAbs with low affinity for mMOG were not used in these studies. mAbs 1002, 1003, 1011, 1012, and 1022 competed for binding to mMOG, whereas mAbs 1004, 1005, 1009, 1010, and 1023 did not (Fig. 2 and data not shown). However, the lack of dependence of competing Abs for residues 103 and 104 in the FG loop for recognition indicates that binding of 8-18C5 to mMOG inhibits interactions with these Abs through either steric effects or binding to a partially overlapping epitope.

*Immunization of mice with mMOG or hMOG results in a polyclonal Ab response that is not affected by mutation of FG loop residues*

Based on earlier observations (7), the lack of dependence of the MOG-specific Abs on residues 103 and 104 for recognition was unexpected. It was therefore important to assess whether the mAbs generated in response to hMOG immunization were representative of the polyclonal response. C57BL/6 mice were immunized with hMOG and, for comparative purposes, mMOG. Humoral responses against hMOG, mMOG, and mMOG-DM were assessed using ELISAs on days 8, 11, and 13 postimmunization (Fig. 3A and data not shown). Immunization of mice with either hMOG or mMOG results in a response that is not ablated by mutation of residues 103 and 104 (Fig. 3A). Although there were slight decreases and increases in ELISA signals in hMOG- and mMOG-immunized mice, respectively, for binding to mMOG-DM relative to mMOG, these differences were statistically significant in some mice, but not others, within the groups. In addition, the Ab response induced by hMOG immunization resulted in higher ELISA signals for both hMOG and mMOG recognition relative to that following mMOG immunization (Fig. 3A). To ensure that the ELISA signals in Fig. 3A were not saturating for hMOG-immunized mice, the use of higher serum dilutions also demonstrated that recognition of mMOG is not dependent on residues 103 and 104 (Fig. 3B).

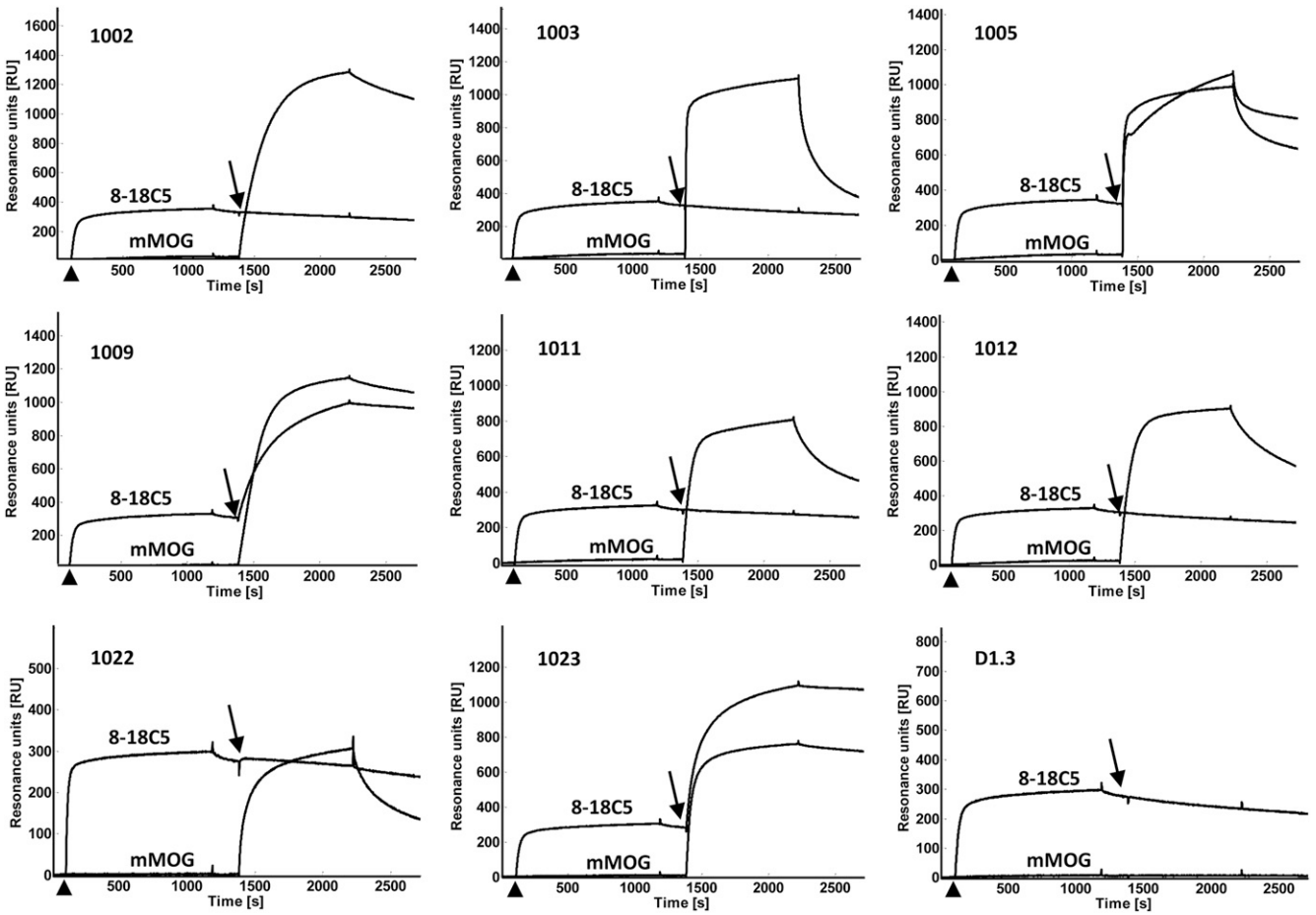


**FIGURE 2.** SPR assays to assess competition of mAbs with 8-18C5 for binding to recombinant mMOG. mAb 8-18C5 and mMOG were immobilized on two flow cells of a CM5 sensor chip. mMOG (5 μg/ml; ~200 nM) was injected (arrowhead) followed by mAb (arrow). Each mAb was injected at a concentration of ~5-fold its $K_d$ value for interaction with mMOG. Overlaid sensorgrams are shown for the 8-18C5 coupled flow cell (showing mMOG binding followed by mAb binding if the mAb does not compete with 8-18C5) and the mMOG coupled flow cell (showing only mAb binding as a control). The anti-lysozyme Ab D1.3 (35) was used as a control (*bottom right panel*). Data are representative of at least two injections for each mAb.

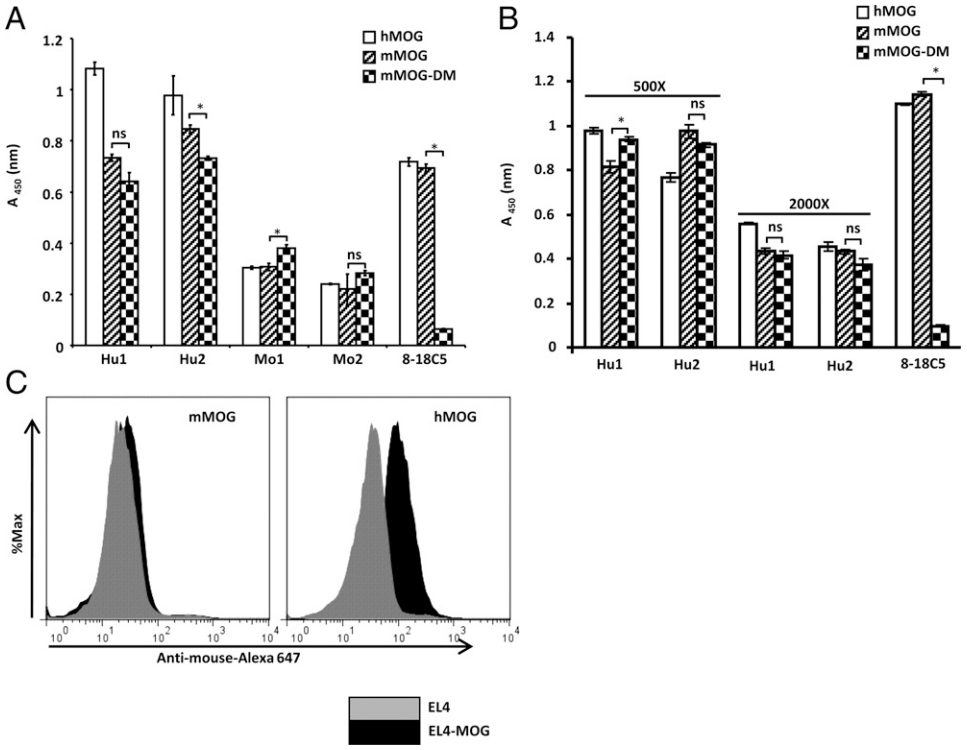


**FIGURE 3.** Humoral responses in hMOG- and mMOG-immunized C57BL/6 mice are not dependent on residues 103 and 104 of the FG loop of MOG for recognition but the two immunogens induce Abs that differ in their ability to recognize mMOG expressed on the surface of transfected EL-4 cells (EL4-MOG cells). (**A** and **B**) Sera [1:250 dilutions for (A); 1:500, 1:2,000 dilutions for (B)] harvested at day 13 postimmunization were analyzed for binding by ELISA. Data shown are derived from representative mice from each group ($n = 4$ mice/immunogen; Hu1, Hu2 for hMOG; Mo1, Mo2 for mMOG). Means of triplicate values with SEM are shown. 8-18C5 mAb was used as a control in the ELISAs. (**C**) EL4-MOG cells (transfected to express mMOG) or as control, untransfected EL4 cells, were incubated with 1:100 dilutions of pooled sera isolated at day 22 from immunized mice (4 mice/group). Bound Abs were detected using an Alexa 647–labeled anti-mouse IgG (H + L chain–specific) conjugate. Data are representative of two independent experiments. *$p < 0.05$ (Student $t$ test).

We also used flow cytometry to analyze the ability of the Abs in the serum of immunized mice to bind to mMOG expressed on the surface of transfected EL-4 cells (23). Consistent with the findings of others that rodent MOG immunization of C57BL/6 results in a response that does not recognize native MOG (22, 26), incubation of EL4-MOG cells with Abs from mMOG-immunized mice leads to a very small shift in fluorescence signal relative to the signal observed with untransfected EL4 cells (Fig. 3C). By contrast, hMOG immunization generated Abs that recognize surface expressed MOG (Fig. 3C).

*Exacerbation of EAE by the mAbs in a mouse transfer model*

To assess the encephalitogenicity of the mAbs, we developed a mouse transfer model. This model is distinct from an earlier model because it involves the immunization of wild-type C57BL/6 mice rather than B cell–deficient mice (22, 28) with hMOG35–55 to induce a MOG-specific T cell response followed by the transfer of Abs. Wild-type mice were used as recipients to avoid possible effects of B cell deficiency, such as those resulting from the absence of regulatory B cells. Shortly after disease onset (day 15), mice with similar history of clinical disease score range, mean, and median (8 mice/group; mean disease score for each group of ~2) were computationally assigned to groups and injected with 200 μg test mAb(s), 200 μg isotype control Ab [mouse IgG1 anti-lysozyme D1.3 (35)], or PBS (Fig. 4). In some cases, anti-MOG mAbs that did not exacerbate disease also served as negative controls. We observed no difference in disease course between mice injected with isotype control and DPBS, and these controls were therefore used interchangeably. In most experiments, 8-18C5 was also used because this mAb has been shown in multiple rodent models to have demyelinating activity (17, 21).

With the exception of mAb 1022, all other mAbs that competed with 8-18C5 in the SPR assay exacerbated EAE (Fig. 4). These mAbs are of the IgG1 isotype. In addition, delivery of mAb 1005 that does not compete with 8-18C5 resulted in disease exacerbation that was significantly lower than that observed for mAbs 1002, 1003, 1011, 1012, and 8-18C5 (Fig. 4 and data not shown). Although mAb 1023 delivery resulted in a slight increase in disease activity relative to that in control groups, this difference was not significant (Fig. 4B and data not shown). mAbs 1004, 1009, and 1010 also did not exacerbate EAE (Fig. 4C, 4E, and data not shown).

With the goal of correlating encephalitogenicity with the recognition of native MOG, we used flow cytometry to analyze the binding of the mAbs to EL4-MOG cells (23). Similar assays have been used previously and shown to yield correlations (8, 15, 23, 26, 50). However, although the encephalitogenic mAbs 1002, 1005, 1011, and 1012 bind to these cells, mAb 1003 does not (Fig. 5). Further, mAb 1022 binds well but does not exacerbate EAE. As an alternative approach toward obtaining an in vitro indicator of encephalitogenicity, we also assessed binding of the Abs to mouse CNS sections (Fig. 6). An Ab specific for the O1 marker (galactocerebroside) on mature differentiated OLs was used to detect OLs (Fig. 6A, 6B). This Ab binds to the OL cell body in rodents more strongly than the myelin sheath (51), resulting in punctate staining that does not show extensive overlap with the more diffuse staining patterns seen for the encephalitogenic mAbs (Fig. 6A, 6B). Importantly, incubation of spinal cord sections with the well-characterized mAb, 8-18C5, resulted in a staining pattern that is similar to that of mAbs 1002, 1003, 1005, 1011, and 1012 (Supplemental Fig. 2; background staining levels by mAb 1023 are shown as a control). By contrast with the data shown in Supplemental Fig. 2, the images shown in Fig. 6A and 6B are presented to allow comparisons of relative staining intensities by the different mAbs to be made. Consequently, these images are representative of the quantitative intensity analyses shown in Fig. 6C. In addition, the mAbs bind to myelin-rich regions at higher levels than to myelin-poor regions (Fig. 6, Supplemental Fig. 2, and data not shown).

The mAbs (1002, 1003, 1011, and 1012) with the highest encephalitogenicity gave the strongest staining (Fig. 6). mAbs 1005 and 1022 resulted in relatively low levels of staining (Fig. 6B, 6C). Incubation with all of other mAbs resulted in background

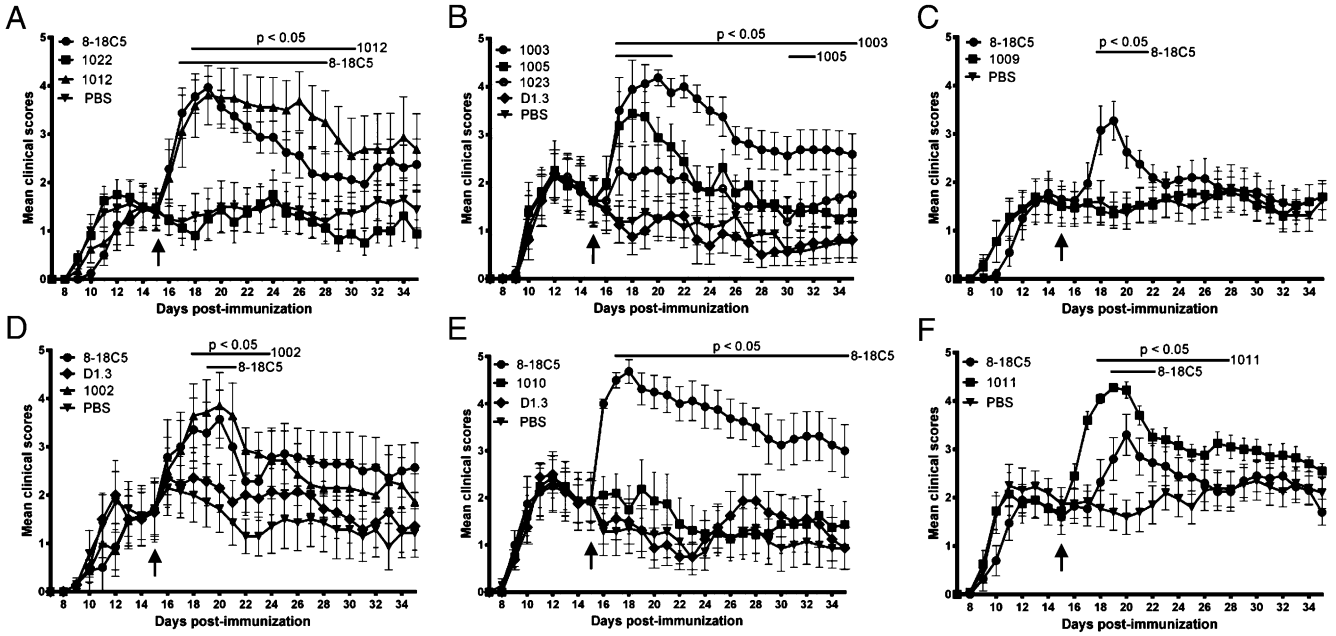


**FIGURE 4.** A subset of the mAbs exacerbates EAE in hMOG35–55 immunized C57BL/6 mice (**A**–**F**). Mice were immunized s.c. with 100 μg hMOG35–55 on day 0 and treated with 200 ng pertussis toxin i.p. on days 0 and 2. On day 15 postimmunization, mice with similar disease score range, mean, and median (8 mice/group; mean disease score for each group of ~2) were divided into groups and injected i.v. with 200 μg mAb, 8-18C5 (control), isotype control (mouse IgG1 anti-lysozyme Ab D1.3), or PBS. Disease was scored for the following 20 d. Error bars indicate SEMs. Days on which statistically significant differences ($p < 0.05$; Student $t$ test for pairwise comparison of groups) were observed between the mean disease scores for mAb-treated and PBS-treated groups are indicated by bars labeled with the corresponding mAb. Data are representative of at least two independent experiments for each mAb.

signal levels (Figs. 6B, 6C). Similar observations were made when spinal cord sections isolated from mice with EAE were incubated with labeled mAbs (data not shown). Of the mAbs (mAbs 1005 and 1022) that bind relatively weakly to CNS sections, only mAb 1005 exacerbates disease following transfer into hMOG35–55-immunized mice (Fig. 4B). This mAb is of the IgG2b isotype, which is more active in effector functions involving FcγRs and/or C1q than mAbs of the IgG1 isotype (52, 53).

mAbs 1002, 1003, 1011, and 1012 compete with 8-18C5 for binding to MOG (Fig. 2), allowing us to further assess the specificity of MOG binding by these mAbs to spinal cord sections by preincubation of the tissue with 8-18C5. This treatment resulted in substantial reductions in staining levels by the mAbs (Fig. 7A, 7B). By contrast, coincubation of spinal cord sections with 8-18C5 and mAb 1005, which bind to distinct epitopes on MOG (Fig. 2), demonstrated that mAb 1005 colocalizes with 8-18C5 (Fig. 7C).

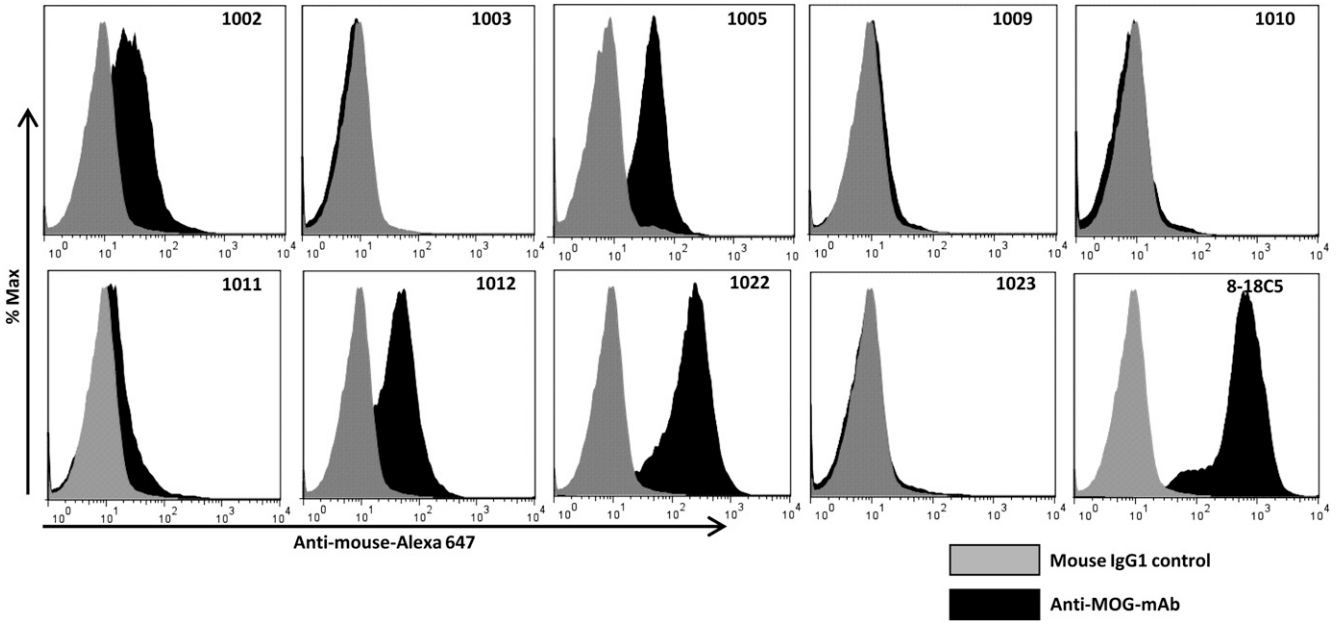


**FIGURE 5.** A subset of the mAbs bind to mMOG expressed on the surface of transfected EL-4 cells. EL4-MOG cells (23) were incubated with 50 μg/ml mAb (black) or, as control, anti-lysozyme D1.3 Ab (mouse IgG1; gray). Bound Abs were detected using an Alexa 647–labeled anti-mouse IgG (H + L chain–specific) conjugate. Data are representative of three independent experiments.

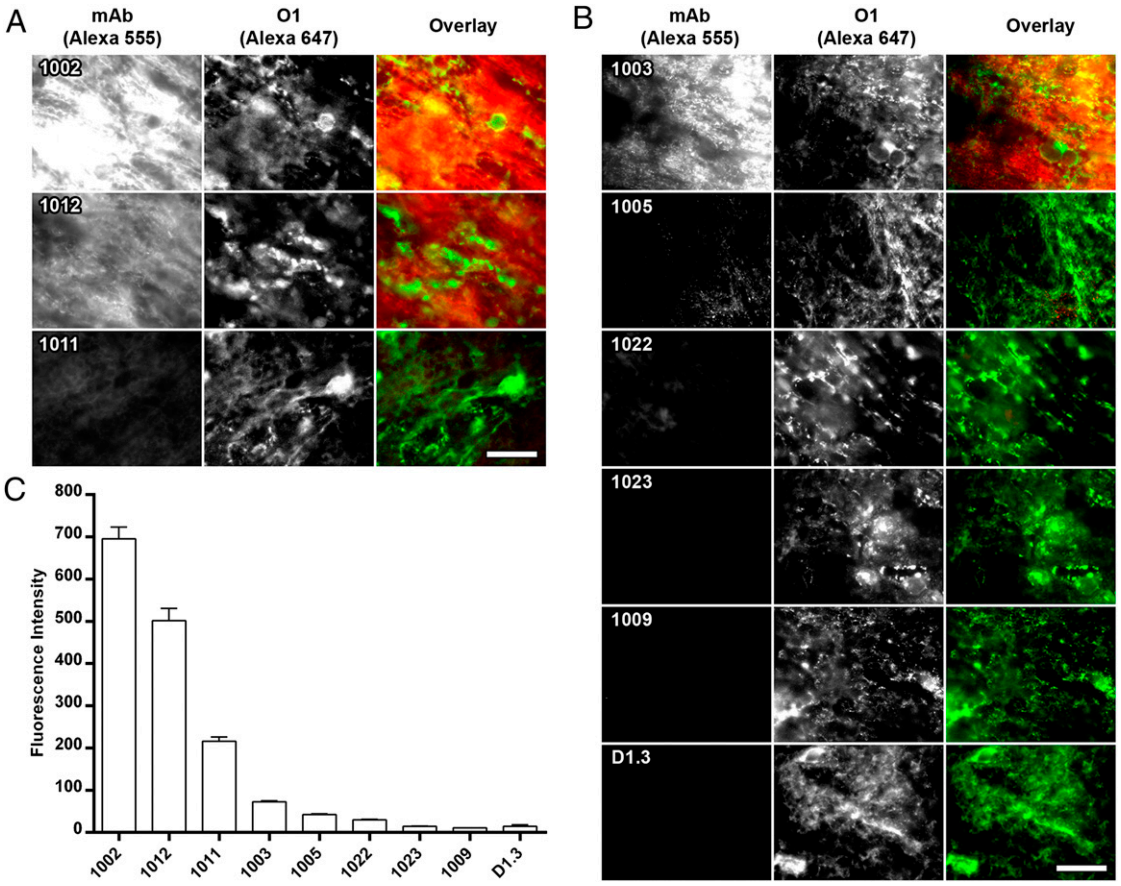


**FIGURE 6.** mAbs with disease-exacerbating activity bind to CNS sections. Spinal cord sections from C57BL/6 mice were costained with 50 μg/ml of Alexa 555–labeled mAbs (pseudocolored red in overlay) and Alexa 647–labeled anti-OL marker O1 (pseudocolored green in overlay). The staining intensities for the mAbs shown in (**A**) were higher than the intensities for mAbs in (**B**). Intensities for Alexa 555–labeled mAbs were adjusted equally within each panel to enable staining intensity differences (**C**) to be visualized. Data are representative of at least three independent experiments. Scale bars, 20 μm. (C) The intensities of the fluorescence staining of spinal cord sections by Alexa 555–labeled mAbs. The difference between the 10th and 80th percentile pixel intensity value for staining by each mAb was calculated and the median value plotted. At least 20 images were acquired for each mAb. Error bars represent SEM.

Thus, all encephalitogenic mAbs either directly compete for binding or colocalize with 8-18C5 in spinal cord sections, demonstrating their specificity for myelin-associated MOG. Consistent with their MOG specificity, the mAbs stained liver sections at background levels that were similar to those observed with the anti-lysozyme mAb D1.3 (data not shown).

To further characterize the epitope specificity of the mAbs that exacerbate EAE, competition assays using SPR were carried out using an analogous approach to that described for Fig. 2. mAbs 1002, 1003, 1011, and 1012, which compete with 8-18C5 (Fig. 2), also block the binding of each other to MOG, whereas mAb 1005 does not compete with these mAbs for interaction with MOG (data not shown). A summary of the binding properties of the mAbs and their ability to exacerbate EAE is presented in Table II. Collectively, our data indicate that the staining of CNS sections, but not other binding assays, is a predictive indicator of encephalitogenicity.

## Discussion

In the current study we have analyzed the properties of MOG-specific mAbs elicited in mice following immunization with recombinant hMOG. Although earlier studies had led to the conclusion that demyelinating MOG-specific humoral responses are focused on two residues (residues 103 and 104) in the exposed FG loop of MOG following immunization of BALB/c or SJL/J mice with rodent or bovine MOG (7), our studies show that this is not the case for hMOG-immunized C57BL/6 mice. Importantly, mAbs that based on their in vitro properties recognize at least four distinct epitopes (represented by mAbs 1003, 1005, 1011, and 1002/1012) are able to exacerbate EAE in a transfer model. By analogy, recent studies in humans have suggested that the pathogenic MOG-specific Ab response is directed toward multiple epitopes that are distinct from the epitope recognized by 8-18C5 (4). Our studies in hMOG-immunized C57BL/6 mice therefore have implications for understanding the disease process in a mouse model of Ab-mediated EAE, which in turn could have relevance to MS.

Much interest has focused on characterizing MOG-specific Abs in humans and mice (3, 4, 7–14). To date, it has been difficult to obtain correlations between pathogenicity and binding properties of Abs. This is particularly so in humans, in whom interaction assays with different forms of Ag have led to inconsistencies (3, 4, 8, 10, 15). Although binding of anti-MOG Abs to MOG-expressing transfectants has been reported to correlate with recognition of native MOG in the CNS (8, 15, 23, 26, 50), we observe that this is not always the case. For example, mAb 1003 binds to CNS sections but not to MOG-transfected EL4 cells, whereas mAb 1022 binds strongly to EL4-MOG cells but at almost background levels to CNS sections. In addition, interactions of the mAbs with recombinant mMOG in either ELISAs or SPR does not

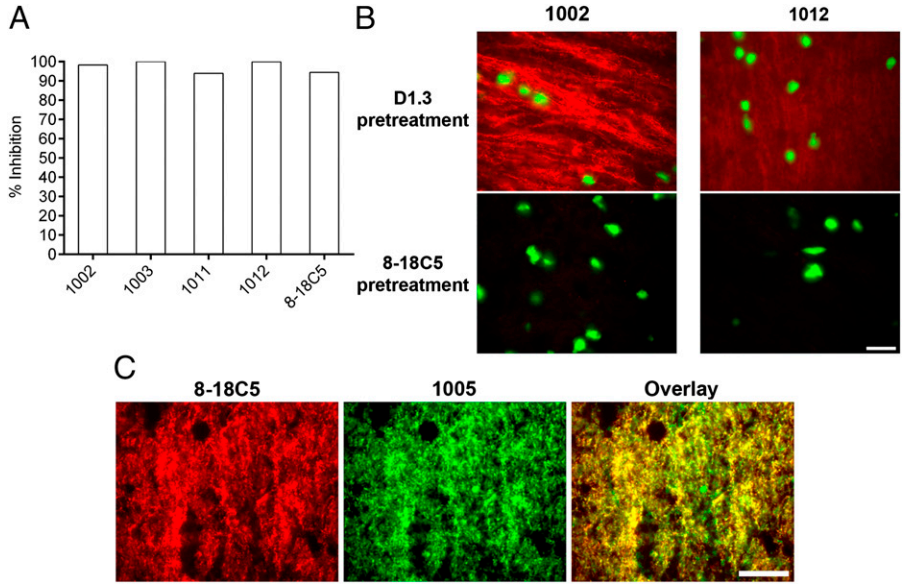


**FIGURE 7.** mAbs 1002, 1003, 1011, and 1012 compete with 8-18C5 for binding to spinal cord sections, whereas mAb 1005 shows extensive colocalization with 8-18C5. (**A**) Spinal cord sections were incubated with 200 μg/ml 8-18C5 or anti-lysozyme D1.3 (isotype control) prior to addition of 50 μg/ml Alexa 555–labeled mAb (including 8-18C5 as a control). Staining intensities with 8-18C5 or D1.3 pretreatment were determined, background subtracted, and inhibition of binding by 8-18C5 relative to control (D1.3) calculated. (**B**) Representative images of spinal cord sections treated as in (A). For each mAb, images with 8-18C5 or D1.3 pretreatment were acquired using the same settings and processed analogously. Alexa Fluor 555 and DAP1 fluorescence are pseudocolored red and green, respectively. Scale bar, 20 μm. (**C**) Spinal cord sections were coincubated with 5 μg/ml Alexa 555–labeled 8-18C5 (pseudocolored red) and 50 μg/ml Alexa 647–labeled mAb 1005 (pseudocolored green). Staining intensities for 8-18C5 and 1005 were adjusted to allow colocalization to be assessed. Data are representative of two experiments. Scale bar, 20 μm.

correlate with encephalitogenicity. A possible reason for this is that a subset of epitopes on soluble recombinant MOG (extracellular domain) are masked in the transmembrane-linked, native form of this protein. Nevertheless, all Abs that bind to CNS sections with a relatively strong signal are able to exacerbate EAE in a transfer model in which mAbs are delivered into C57BL/6 mice with mild disease induced by immunization with the peptide encompassing residues 35–55 of hMOG. In addition, one mAb (1005) of the proinflammatory IgG2b isotype (52) interacts relatively weakly with CNS sections and exacerbates EAE in this model.

Our studies reveal that there are distinct epitopes on MOG that can be recognized by pathogenic, MOG-specific mAbs: first, an epitope recognized by mAbs 1002 and 1012 that partially overlaps with the 8-18C5 epitope and is present on mMOG-transfected EL-4 cells. At this point, 1002 and 1012 have very similar properties in all assays, but it remains possible that their fine epitope specificity is distinct. Second, although 1011 resembles 1002 or 1012 insofar as it competes with 8-18C5 for binding and recognizes EL4-MOG cells, this mAb has a higher affinity for recombinant hMOG relative to mMOG (by SPR), whereas 1002/1012 have similar affinities. Third, mAb 1003 competes with 8-18C5 for binding to recombinant MOG but does not interact with EL4-MOG cells. Fourth, mAb 1005 does not compete with 8-18C5 but binds to EL4-MOG cells. Further, mAbs 1002, 1003, 1011, and 1012 but not mAb 1005 compete with each other for binding to MOG. Combined with their different binding properties, this suggests that 1002/1012, 1003, and 1011 interact with MOG epitopes that are spatially close but not directly overlapping. Indeed, the relatively small size of the single Ig-like extracellular domain of MOG would limit the number of noncompeting mAbs that can bind to this Ag. By contrast with demyelinating mAbs such as 8-18C5 in other mouse models (7), none of the Abs described in this study are dependent on residues 103 and 104 of the FG loop for binding. Structural studies of the 8-18C5 mAb bound to rMOG have shown that although 65% of the interaction surface encompasses the FG loop,

Table II. Properties of the MOG-specific mAbs

| mAb | Isotype | Exacerbation of EAE[a] | CNS Staining[a] | Staining EL4-MOG[a] | ELISA (mMOG)[a] | $K_d$ (nM)[b] (mMOG) | $K_d$ (nM)[b] (mMOG-DM) |
|---|---|---|---|---|---|---|---|
| 1002 | IgG1 | ++ | ++++++ | ++ | ++++ | 4.5 | 5.0 |
| 1003 | IgG1 | ++ | +++ | − | + | 17.0 | 21.0 |
| 1004 | IgG2b | − | ND | − | +++ | 5.4 | 4.2 |
| 1005 | IgG2b | + | ++ | +++ | ++ | 301.0 | 321.0 |
| 1009 | IgG2b | − | − | − | ++++ | 1.0 | 1.5 |
| 1010 | IgG1 | − | − | − | +++++ | 0.9 | 0.5 |
| 1011 | IgG1 | ++ | ++++ | + | +++ | 7.5 | 8.7 |
| 1012 | IgG1 | ++ | +++++ | +++ | ++++ | 3.4 | 3.4 |
| 1022 | IgG1 | − | + | ++++ | +++ | 37.0 | 39.0 |
| 1023 | IgG1 | − | − | − | +++++ | 1.0 | 1.2 |

[a]Numbers of + signs indicate the relative activities of mAbs; − indicates no activity.
[b]Values also shown in Table I.
ND, Not determined.

the BC and C'C'' loops also contribute to binding (34). Thus, the mAbs that compete with 8-18C5 most likely interact with residues in one or more of these other loops, and/or FG loop residues that do not include aa 103 or 104. Alternatively, longer range steric effects could also be operative.

Significantly, immunization of C57BL/6 mice with hMOG or mMOG results in a polyclonal response that is independent of residues 103 or 104 for recognition, indicating that the hybridoma Abs are representative of the repertoire. The reason for this difference in dependence on these residues between BALB/c or SJL/J and C57BL/6 mice is not clear, but may relate to the variations in mouse strain and immunization approach (7). Specifically, in these earlier studies, immunizations included the use of partially purified rMOG or bovine MOG or delivery of an mMOG expression plasmid via genetic vaccination (7, 17, 20). By contrast with BALB/c or SJL/J mice, immunization of C57BL/6 mice with recombinant rMOG/mMOG results in a humoral response that does not recognize native MOG (22, 26, and this study). This difference has been proposed to be due to genetic variations mapping to the MHC class II locus (26). However, the observation that hMOG immunization results in Ab-mediated EAE and that the variation in encephalitogenicity of the humoral response can be mapped to a single amino acid difference at position 42 (Ser in rodent MOG; Pro in hMOG) within the immunodominant T cell epitope suggest that the distinct behavior is most likely related to a qualitative difference in MOG35–55-specific T cell responses (22, 27).

The recognition of noncompeting epitopes of MOG by Abs in hMOG-immunized mice has implications for disease pathogenesis, because it would enable extensive cross linking of MOG on the OLs. Ab-mediated cross linking has been shown in earlier studies to induce repartitioning of MOG into lipid rafts and changes in OL morphology that could be early contributors to demyelination (32, 33). Further, immune complex formation by polyspecific Abs with MOG (fragments) released under inflammatory conditions in the CNS could impact the (re)presentation of Ag to infiltrating autoreactive $CD4^+$ T cells.

Although complement deposits have been observed in the CNS of MS patients (29, 54, 55), mouse IgG1 does not bind well to the complement component, C1q (53), and yet four of the five pathogenic mAbs characterized in this study are of this isotype. This suggests that FcγR interactions with infiltrating macrophages and resident microglia play an important role in pathogenesis in mice. In this context, mouse IgG1 binds with higher affinity to the inhibitory FcR, FcγRIIb, than to the activating receptor FcγRIII and does not interact with activating FcγRI or FcγRIV (52, 56). However, during inflammation, FcγRIII expression levels can increase whereas FcγRIIb levels decrease, leading to inflammatory signaling by IgG1 (57, 58). By contrast with mouse IgG1, mouse IgG2b can bind to complement C1q (53) and also has higher affinity for activating FcγRs (FcγRI, FcγRIII, and FcγRIV) relative to the inhibitory FcγRIIb (52, 57). Consequently, Abs of the IgG2b class that bind to native MOG are expected to be more damaging to the CNS than their IgG1 counterparts. Consistent with this, despite the relatively low affinity of mAb 1005 for mMOG (~300 nM by SPR) and weak binding to CNS sections, this mAb is able to exacerbate EAE following transfer into hMOG35–55-immunized mice. By contrast, encephalitogenic Abs of the IgG1 subclass bind at higher levels to CNS sections.

Collectively, our studies demonstrate that the pathogenic humoral response in mice following immunization with hMOG is diverse, with multiple epitopes being targeted. This contrasts with the focused response that has been described in other rodent models (7), but could be analogous to the recent demonstration that pathogenic Abs are directed toward multiple MOG epitopes in human MS samples (4). Further, despite relatively low affinity for MOG, an mAb of the highly inflammatory isotype IgG2b (52, 53, 57) can exacerbate EAE. Combined with analyses indicating that the humoral response in patients with MS is characterized by low-affinity Abs (59), this suggests that the threshold binding levels for CNS damage can be low, particularly if the Ab is of a proinflammatory isotype. Our studies not only reveal novel epitopes for MOG recognition in the CNS, but could also have relevance to understanding how the humoral response contributes to MS.

## Acknowledgments

We thank Dr. Gurumoorthy Krishnamoorthy (Max Planck Institute of Neurobiology) and Drs. Anne Cross and Jerry Lyons (Washington University, St. Louis, MO) for generously providing EL4 cells expressing mouse MOG and baculoviral stocks to express recombinant hMOG, respectively. We also thank Dr. Sripad Ram for expert assistance with microscopy experiments, Alberto Puig-Canto for help with SPR experiments, and Dr. Stephen Anthony for developing a computational algorithm for mouse grouping.

## Disclosures

The authors have no financial conflicts of interest.

## References

1. Popescu, B. F., and C. F. Lucchinetti. 2012. Pathology of demyelinating diseases. *Annu. Rev. Pathol.* 7: 185–217.
2. Hafler, D. A., J. M. Slavik, D. E. Anderson, K. C. O'Connor, P. De Jager, and C. Baecher-Allan. 2005. Multiple sclerosis. *Immunol. Rev.* 204: 208–231.
3. Menge, T., H. C. von Büdingen, P. H. Lalive, and C. P. Genain. 2007. Relevant antibody subsets against MOG recognize conformational epitopes exclusively exposed in solid-phase ELISA. *Eur. J. Immunol.* 37: 3229–3239.
4. Menge, T., P. H. Lalive, H. C. von Büdingen, and C. P. Genain. 2011. Conformational epitopes of myelin oligodendrocyte glycoprotein are targets of potentially pathogenic antibody responses in multiple sclerosis. *J. Neuroinflammation* 8: 161.
5. Brunner, C., H. Lassmann, T. V. Waehneldt, J. M. Matthieu, and C. Linington. 1989. Differential ultrastructural localization of myelin basic protein, myelin/oligodendroglial glycoprotein, and 2′,3′-cyclic nucleotide 3′-phosphodiesterase in the CNS of adult rats. *J. Neurochem.* 52: 296–304.
6. Johns, T. G., and C. C. Bernard. 1999. The structure and function of myelin oligodendrocyte glycoprotein. *J. Neurochem.* 72: 1–9.
7. Breithaupt, C., B. Schäfer, H. Pellkofer, R. Huber, C. Linington, and U. Jacob. 2008. Demyelinating myelin oligodendrocyte glycoprotein-specific autoantibody response is focused on one dominant conformational epitope region in rodents. *J. Immunol.* 181: 1255–1263.
8. Zhou, D., R. Srivastava, S. Nessler, V. Grummel, N. Sommer, W. Brück, H. P. Hartung, C. Stadelmann, and B. Hemmer. 2006. Identification of a pathogenic antibody response to native myelin oligodendrocyte glycoprotein in multiple sclerosis. *Proc. Natl. Acad. Sci. USA* 103: 19057–19062.
9. Berger, T., P. Rubner, F. Schautzer, R. Egg, H. Ulmer, I. Mayringer, E. Dilitz, F. Deisenhammer, and M. Reindl. 2003. Antimyelin antibodies as a predictor of clinically definite multiple sclerosis after a first demyelinating event. *N. Engl. J. Med.* 349: 139–145.
10. Reindl, M., M. Khalil, and T. Berger. 2006. Antibodies as biological markers for pathophysiological processes in MS. *J. Neuroimmunol.* 180: 50–62.
11. von Büdingen, H.-C., S. L. Hauser, A. Fuhrmann, C. B. Nabavi, J. I. Lee, and C. P. Genain. 2002. Molecular characterization of antibody specificities against myelin/oligodendrocyte glycoprotein in autoimmune demyelination. *Proc. Natl. Acad. Sci. USA* 99: 8207–8212.
12. O'Connor, K. C., H. Appel, L. Bregoli, M. E. Call, I. Catz, J. A. Chan, N. H. Moore, K. G. Warren, S. J. Wong, D. A. Hafler, and K. W. Wucherpfennig. 2005. Antibodies from inflamed central nervous system tissue recognize myelin oligodendrocyte glycoprotein. *J. Immunol.* 175: 1974–1982.
13. Owens, G. P., J. L. Bennett, H. Lassmann, K. C. O'Connor, A. M. Ritchie, A. Shearer, C. Lam, X. Yu, M. Birlea, C. DuPree, et al. 2009. Antibodies produced by clonally expanded plasma cells in multiple sclerosis cerebrospinal fluid. *Ann. Neurol.* 65: 639–649.
14. Cameron, E. M., S. Spencer, J. Lazarini, C. T. Harp, E. S. Ward, M. Burgoon, G. P. Owens, M. K. Racke, J. L. Bennett, E. M. Frohman, and N. L. Monson. 2009. Potential of a unique antibody gene signature to predict conversion to clinically definite multiple sclerosis. *J. Neuroimmunol.* 213: 123–130.
15. Lalive, P. H., T. Menge, C. Delarasse, B. Della Gaspera, D. Pham-Dinh, P. Villoslada, H. C. von Büdingen, and C. P. Genain. 2006. Antibodies to native myelin oligodendrocyte glycoprotein are serologic markers of early inflammation in multiple sclerosis. *Proc. Natl. Acad. Sci. USA* 103: 2280–2285.
16. Gaertner, S., K. L. de Graaf, B. Greve, and R. Weissert. 2004. Antibodies against glycosylated native MOG are elevated in patients with multiple sclerosis. *Neurology* 63: 2381–2383.

17. Linnington, C., M. Webb, and P. L. Woodhams. 1984. A novel myelin-associated glycoprotein defined by a mouse monoclonal antibody. *J. Neuroimmunol.* 6: 387–396.
18. Brehm, U., S. J. Piddlesden, M. V. Gardinier, and C. Linington. 1999. Epitope specificity of demyelinating monoclonal autoantibodies directed against the human myelin oligodendrocyte glycoprotein (MOG). *J. Neuroimmunol.* 97: 9–15.
19. Bourquin, C., A. Iglesias, T. Berger, H. Wekerle, and C. Linington. 2000. Myelin oligodendrocyte glycoprotein-DNA vaccination induces antibody-mediated autoaggression in experimental autoimmune encephalomyelitis. *Eur. J. Immunol.* 30: 3663–3671.
20. Piddlesden, S. J., H. Lassmann, F. Zimprich, B. P. Morgan, and C. Linington. 1993. The demyelinating potential of antibodies to myelin oligodendrocyte glycoprotein is related to their ability to fix complement. *Am. J. Pathol.* 143: 555–564.
21. Schluesener, H. J., R. A. Sobel, C. Linington, and H. L. Weiner. 1987. A monoclonal antibody against a myelin oligodendrocyte glycoprotein induces relapses and demyelination in central nervous system autoimmune disease. *J. Immunol.* 139: 4016–4021.
22. Marta, C. B., A. R. Oliver, R. A. Sweet, S. E. Pfeiffer, and N. H. Ruddle. 2005. Pathogenic myelin oligodendrocyte glycoprotein antibodies recognize glycosylated epitopes and perturb oligodendrocyte physiology. *Proc. Natl. Acad. Sci. USA* 102: 13992–13997.
23. Pöllinger, B., G. Krishnamoorthy, K. Berer, H. Lassmann, M. R. Bösl, R. Dunn, H. S. Domingues, A. Holz, F. C. Kurschus, and H. Wekerle. 2009. Spontaneous relapsing-remitting EAE in the SJL/J mouse: MOG-reactive transgenic T cells recruit endogenous MOG-specific B cells. *J. Exp. Med.* 206: 1303–1316.
24. Lyons, J. A., M. San, M. P. Happ, and A. H. Cross. 1999. B cells are critical to induction of experimental allergic encephalomyelitis by protein but not by a short encephalitogenic peptide. *Eur. J. Immunol.* 29: 3432–3439.
25. Hjelmström, P., A. E. Juedes, J. Fjell, and N. H. Ruddle. 1998. B-cell-deficient mice develop experimental allergic encephalomyelitis with demyelination after myelin oligodendrocyte glycoprotein sensitization. *J. Immunol.* 161: 4480–4483.
26. Bourquin, C., A. Schubart, S. Tobollik, I. Mather, S. Ogg, R. Liblau, and C. Linington. 2003. Selective unresponsiveness to conformational B cell epitopes of the myelin oligodendrocyte glycoprotein in H-2b mice. *J. Immunol.* 171: 455–461.
27. Oliver, A. R., G. M. Lyon, and N. H. Ruddle. 2003. Rat and human myelin oligodendrocyte glycoproteins induce experimental autoimmune encephalomyelitis by different mechanisms in C57BL/6 mice. *J. Immunol.* 171: 462–468.
28. Lyons, J. A., M. J. Ramsbottom, and A. H. Cross. 2002. Critical role of antigen-specific antibody in experimental autoimmune encephalomyelitis induced by recombinant myelin oligodendrocyte glycoprotein. *Eur. J. Immunol.* 32: 1905–1913.
29. Storch, M. K., S. Piddlesden, M. Haltia, M. Iivanainen, P. Morgan, and H. Lassmann. 1998. Multiple sclerosis: in situ evidence for antibody- and complement-mediated demyelination. *Ann. Neurol.* 43: 465–471.
30. Raine, C. S., B. Cannella, S. L. Hauser, and C. P. Genain. 1999. Demyelination in primate autoimmune encephalomyelitis and acute multiple sclerosis lesions: a case for antigen-specific antibody mediation. *Ann. Neurol.* 46: 144–160.
31. Lucchinetti, C., W. Brück, J. Parisi, B. Scheithauer, M. Rodriguez, and H. Lassmann. 2000. Heterogeneity of multiple sclerosis lesions: implications for the pathogenesis of demyelination. *Ann. Neurol.* 47: 707–717.
32. Marta, C. B., M. B. Montano, C. M. Taylor, A. L. Taylor, R. Bansal, and S. E. Pfeiffer. 2005. Signaling cascades activated upon antibody cross-linking of myelin oligodendrocyte glycoprotein: potential implications for multiple sclerosis. *J. Biol. Chem.* 280: 8985–8993.
33. Marta, C. B., C. M. Taylor, T. Coetzee, T. Kim, S. Winkler, R. Bansal, and S. E. Pfeiffer. 2003. Antibody cross-linking of myelin oligodendrocyte glycoprotein leads to its rapid repartitioning into detergent-insoluble fractions, and altered protein phosphorylation and cell morphology. *J. Neurosci.* 23: 5461–5471.
34. Breithaupt, C., A. Schubart, H. Zander, A. Skerra, R. Huber, C. Linington, and U. Jacob. 2003. Structural insights into the antigenicity of myelin oligodendrocyte glycoprotein. *Proc. Natl. Acad. Sci. USA* 100: 9446–9451.
35. Amit, A. G., R. A. Mariuzza, S. E. Phillips, and R. J. Poljak. 1986. Three-dimensional structure of an antigen-antibody complex at 2.8 Å resolution. *Science* 233: 747–753.
36. Horton, R. M., H. D. Hunt, S. N. Ho, J. K. Pullen, and L. R. Pease. 1989. Engineering hybrid genes without the use of restriction enzymes: gene splicing by overlap extension. *Gene* 77: 61–68.
37. Devaux, B., F. Enderlin, B. Wallner, and D. E. Smilek. 1997. Induction of EAE in mice with recombinant human MOG, and treatment of EAE with a MOG peptide. *J. Neuroimmunol.* 75: 169–173.
38. Radu, C. G., S. M. Anderton, M. Firan, D. C. Wraith, and E. S. Ward. 2000. Detection of autoreactive T cells in H-2$^{u}$ mice using peptide-MHC multimers. *Int. Immunol.* 12: 1553–1560.
39. Yokoyama, W. M., M. Christensen, G.D. Santos, and D. Miller. 2006. Production of monoclonal antibodies. *Curr. Protoc.Immunol.* 2.5.1–2.5.25.
40. Foote, J., and G. Winter. 1992. Antibody framework residues affecting the conformation of the hypervariable loops. *J. Mol. Biol.* 224: 487–499.
41. Kabat, E. A., T. T. Wu, H. M. Perry, K. S. Gottesman, and C. Foeller. 1991. *Sequences of Proteins of Immunological Interest*, 5th ed. Bethesda, MD. U.S. Department of Health and Human Services.
42. Ward, E. S., D. Güssow, A. D. Griffiths, P. T. Jones, and G. Winter. 1989. Binding activities of a repertoire of single immunoglobulin variable domains secreted from *Escherichia coli. Nature* 341: 544–546.
43. Clackson, T., H. R. Hoogenboom, A. D. Griffiths, and G. Winter. 1991. Making antibody fragments using phage display libraries. *Nature* 352: 624–628.
44. Ward, E. S. 1995. VH shuffling can be used to convert an Fv fragment of anti-hen egg lysozyme specificity to one that recognizes a T cell receptor V alpha. *Mol. Immunol.* 32: 147–156.
45. Krebber, A., S. Bornhauser, J. Burmester, A. Honegger, J. Willuda, H. R. Bosshard, and A. Plückthun. 1997. Reliable cloning of functional antibody variable domains from hybridomas and spleen cell repertoires employing a reengineered phage display system. *J. Immunol. Methods* 201: 35–55.
46. Ober, R. J., and E. S. Ward. 2002. Compensation for loss of ligand activity in surface plasmon resonance experiments. *Anal. Biochem.* 306: 228–236.
47. Zhou, J., F. Mateos, R. J. Ober, and E. S. Ward. 2005. Conferring the binding properties of the mouse MHC class I-related receptor, FcRn, onto the human ortholog by sequential rounds of site-directed mutagenesis. *J. Mol. Biol.* 345: 1071–1081.
48. Minguela, A., S. Pastor, W. Mi, J. A. Richardson, and E. S. Ward. 2007. Feedback regulation of murine autoimmunity via dominant anti-inflammatory effects of interferon gamma. *J. Immunol.* 178: 134–144.
49. Ober, R. J., C. Martinez, C. Vaccaro, J. Zhou, and E. S. Ward. 2004. Visualizing the site and dynamics of IgG salvage by the MHC class I-related receptor, FcRn. *J. Immunol.* 172: 2021–2029.
50. Haase, C. G., J. Guggenmos, U. Brehm, M. Andersson, T. Olsson, M. Reindl, J. M. Schneidewind, U. K. Zettl, F. Heidenreich, T. Berger, et al. 2001. The fine specificity of the myelin oligodendrocyte glycoprotein autoantibody response in patients with multiple sclerosis and normal healthy controls. *J. Neuroimmunol.* 114: 220–225.
51. Mela, A., and J. E. Goldman. 2009. The tetraspanin KAI1/CD82 is expressed by late-lineage oligodendrocyte precursors and may function to restrict precursor migration and promote oligodendrocyte differentiation and myelination. *J. Neurosci.* 29: 11172–11181.
52. Nimmerjahn, F., and J. V. Ravetch. 2005. Divergent immunoglobulin g subclass activity through selective Fc receptor binding. *Science* 310: 1510–1512.
53. Duncan, A. R., and G. Winter. 1988. The binding site for C1q on IgG. *Nature* 332: 738–740.
54. Lassmann, H., W. Brück, and C. Lucchinetti. 2001. Heterogeneity of multiple sclerosis pathogenesis: implications for diagnosis and therapy. *Trends Mol. Med.* 7: 115–121.
55. Barnett, M. H., J. D. Parratt, E. S. Cho, and J. W. Prineas. 2009. Immunoglobulins and complement in postmortem multiple sclerosis tissue. *Ann. Neurol.* 65: 32–46.
56. Nimmerjahn, F., P. Bruhns, K. Horiuchi, and J. V. Ravetch. 2005. FcgammaRIV: a novel FcR with distinct IgG subclass specificity. *Immunity* 23: 41–51.
57. Nimmerjahn, F., and J. V. Ravetch. 2006. Fcgamma receptors: old friends and new family members. *Immunity* 24: 19–28.
58. Radeke, H. H., I. Janssen-Graalfs, E. N. Sowa, N. Chouchakova, J. Skokowa, F. Löscher, R. E. Schmidt, P. Heeringa, and J. E. Gessner. 2002. Opposite regulation of type II and III receptors for immunoglobulin G in mouse glomerular mesangial cells and in the induction of anti-glomerular basement membrane (GBM) nephritis. *J. Biol. Chem.* 277: 27535–27544.
59. O'Connor, K. C., T. Chitnis, D. E. Griffin, S. Piyasirisilp, A. Bar-Or, S. Khoury, K. W. Wucherpfennig, and D. A. Hafler. 2003. Myelin basic protein-reactive autoantibodies in the serum and cerebrospinal fluid of multiple sclerosis patients are characterized by low-affinity interactions. *J. Neuroimmunol.* 136: 140–148.